Supplementary Information

Facile synthesis of Fe$_3$O$_4$ nanorod decorated reduced graphene oxide (RGO) for supercapacitor application

Ashok Kumar Das[a]*, Sumanta Sahoo[a], Prabhakarn Arunachalam[b], Suojiang Zhang[c] & Jae-Jin Shim[a]*

[a]School of Chemical Engineering, Yeungnam University, Gyeongsan, Gyeongbuk, 712-749, Republic of Korea

[b]Electrochemistry Research Group, Chemistry Department, College of Science, King Saud University, Riyadh 11451, Saudi Arabia.

[c]Institute of Process Engineering, Chinese Academy of Sciences, Beijing 100190, China

Corresponding author: Dr. Ashok Kumar Das

E-mail address: akdschemuu@gmail.com

Co-corresponding author: Dr. Jae-Jin Shim

E-mail address: jjshim@yu.ac.kr
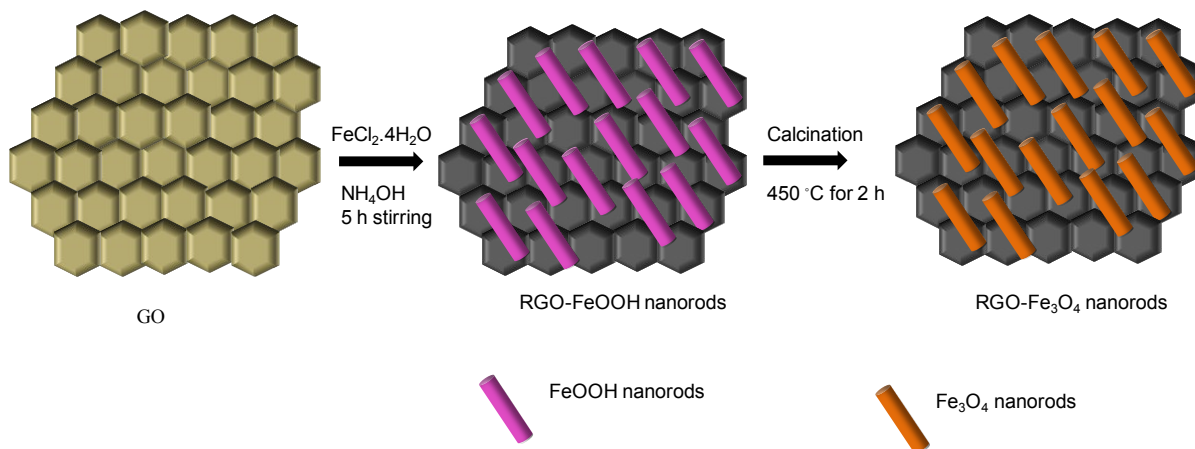
Preparation of graphene oxide (GO)

Graphene oxide (GO) was synthesized by a reported method described elsewhere.[47] Briefly, 2 g of natural graphite flakes were put in a round bottom flask containing 46 mL concentrated H_2SO_4. This round-bottomed flask was transferred to an ice bath with a temperature of approximately 0-5 °C, 6 g of solid $KMnO_4$ was then added slowly, and the mixture was stirred for 2 h. The round-bottomed flask was then transferred to an oil bath pre-heated to 35 °C and was stirred overnight. After that, 90 mL of de-ionized (DI) water was added to it, followed by stirring for another 2 h. Then, a 35% H_2O_2 was added slowly to achieve a bright yellow reaction mixture. The excess manganese salt that was present in the GO was removed using dilute hydrochloric acid (5% by volume). The GO was washed several times and dispersed in water for one month. After one month, the brown precipitate was collected and dried in a vacuum oven.

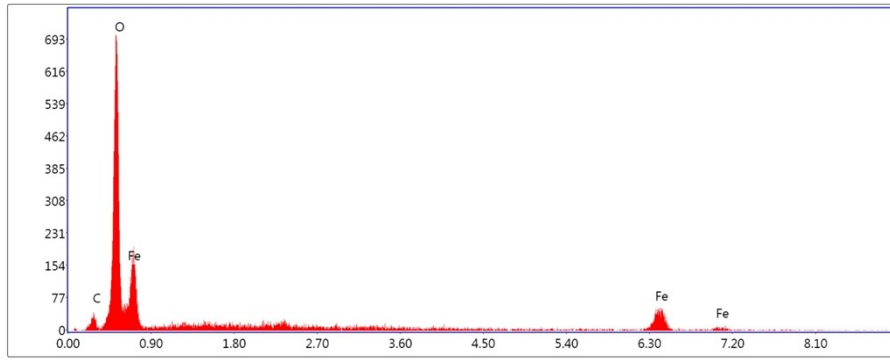**Preparation of the working electrodes**

The Ni-foam (2 cm X 1 cm) was used as a current collector in this investigation. Prior to the use, the Ni-foam was cleaned using 6 M HCl via sonication upto 30 min in order to remove the NiO present on its surface and was washed carefully with DI water to be used as a support for the active electrode material. Typically, the active electrode material dispersion consisting of Fe_3O_4-RGO (60%), PVDF (20%) and carbon black (20%) was prepared using NMP as a solvent and was drop casted onto the Ni-foam substrate followed by drying.

Instrumentation

The structural and morphological analysis of the as-synthesized materials were carried out using X-ray diffraction (PANalytical, X'Pert-PRO MPD, using CuKα radiation), Raman spectroscopy (Renishaw InVia Raman microscope), Brunauer-Emmer-Teller analysis (NOVA 2200e surface area analyser), scanning electron microscopy (Hitachi, S-4200) and high resolution transmission electron microscopy (Philips, CM-200, at an acceleration voltage of 200 kV). All the electrochemical investigations were carried out using potentiostat/galvanostat (Autolab PGSTAT 302N) with a three electrode system. Nickel foam casted with active electrode material, Pt wire and Saturated Calomel Electrode (SCE) were used as working, counter and reference electrodes, respectively. All the electrochemical experiments were performed at room temperature using 1M KOH as electrolyte.
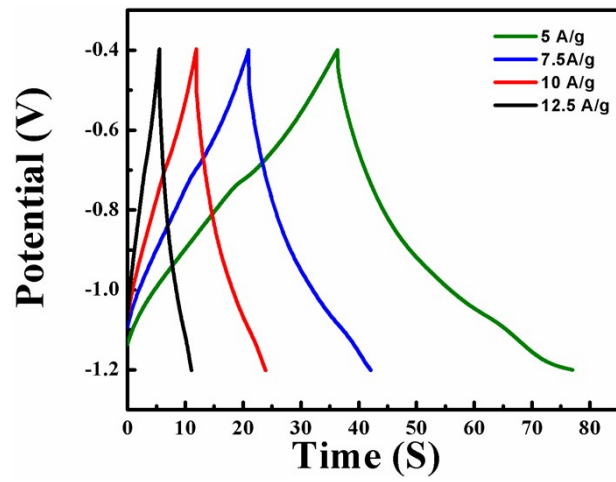
FeCl$_2$.4H$_2$O

NH$_4$OH
5 h stirring

Calcination

450 °C for 2 h

GO

RGO-FeOOH nanorods

RGO-Fe$_3$O$_4$ nanorods

FeOOH nanorods

Fe$_3$O$_4$ nanorods

Scheme S1 Scheme illustrating the synthesis of RGO-Fe$_3$O$_4$ nanocomposite.

Fig.S1 EDS spectrum of RGO-Fe$_3$O$_4$ nanocomposite.
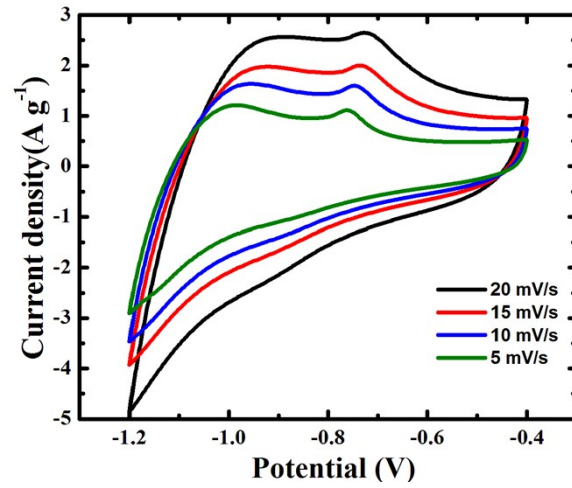
Fig.S2 Cyclic voltammetric response of Fe_3O_4 nanorod based electrode in 1 M KOH at different scan rates.

Fig. S3 Galvanostatic charge-discharge curves of Fe$_3$O$_4$ nanorod based electrode at different current densities.

Table S1 Comparison of the supercapacitor performance of RGO-Fe$_3$O$_4$ nanorod composite with other RGO-Fe$_3$O$_4$ nanocomposite based electrodes.

Structure	Specific surface area(m^{2}g^{-1})	Specific charge storage capacity(Cg^{-1})	Stability	Loading mass(mg)	Refs.
Nanorods	180	315	95% (5 A g^{-1}, 2000 cycles)	6	This work
Quasi-spherical	109	\	60% (100 mVs^{-1}, 10000 cycles)	8	1
Quasi-spherical	151	\	79% (10 A g^{-1}, 1000 cycles)	7.5	2
Quasi-spherical	\	\	95% (10 mVs^{-1}, 1000 cycles)	8	3
Quasi-spherical	\	\	87 (1 A g^{-1}, 500 cycles)	\	4
Quasi-spherical	67.3076	\	(2.3 A g^{-1}, 10 cycles)	0.5	5
Spherical	\	\	67%(2A g^{-1}, 1000 cycles)	8	6
Quasi-qubic	\	\	73% (0.5A g^{-1}, 3000 cycles)	3	7

References

1   T. Qi, J. Jiang, H. Chen, H. Wan, L. Miao and L. Zhang, *Electrochim. Acta,* 2013, **114,** 674-680.

2   L. Li, P. Gao, S. Gai, F. He, Y. Chen, M. Zhang and P. Yang, *Electrochim. Acta,* 2016, **190,** 566-573.

3   L. Li, Y. Dou, L. Wang, M. Luo and Jun Liang RSC Adv., 2014, **4,** 25658–25665

4   S. Ghasemi and F. Ahmadi, *J. Power Sources,* 2015, **289,** 129-137.

5   V. Muthukannan, K. Praveen and B. Natesan, *Mater. Chem. Phys.,* 2015, **162,** 400-407.

6   W. Zhang, F. Liu, Q. Li, Q. Shou, J. Cheng, L. Zhang, B. J. Nelson and X. Zhang, *Phys. Chem. Chem. Phys.,* 2012, **14,** 16331-16337.

7   T. Liu, X. Zhang, B. Li, J. Ding, Y. Liu, G. Li, X. Meng, Q. Caib and J. Zhang, *RSC Adv.,* 2014, **4,** 50765-50770.